Supplemental Data

STIM1 Clusters and Activates

CRAC Channels via Direct Binding

of a Cytosolic Domain to Orai1

Chan Young Park, Paul J. Hoover, Franklin M. Mullins, Priti Bachhawat, Elizabeth D. Covington, Stefan Raunser, Thomas Walz, K. Christopher Garcia, Ricardo E. Dolmetsch, and Richard S. Lewis

SUPPLEMENTAL EXPERIMENTAL PROCEDURES

Materials and Antibodies

2-Aminoethoxydiphenylborate (2-APB) and 3-amino-1,2,4-triazole (3-AT) were obtained from Sigma. Fura-2/AM, Lipofectamine 2000 and 5-bromo-4-chloro-3-indolyl-β-D-galactosidase (X-gal) were obtained from Invitrogen. Thapsigargin and phorbol 12-myristate 13-acetate (PMA) were from LC Laboratories, anti-Flag M2 affinity gel was obtained from Sigma, and Immunopure protein G beads were from Pierce. Antibodies targeting myc (4A6, Upstate), HA (3F10, Roche), GFP (598, MBL), GST (Santa Cruz Biotechnology), and 6xHIS (Qiagen) were purchased from the indicated vendor.

Plasmids

mCh-STIM1 and eGFP-myc-Orai1 plasmids were described previously (Luik et al., 2006). mCh-STIM1-ΔK was constructed by substituting nucleotides at positions 2011 (c→t) and 2013 (g→a) (Quickchange XL; Stratagene) with primer 5'-gactccagcccaggctgaaagaagtttcctctc-3' to generate a premature stop codon. For comparison purposes, YFP-CT-STIM1 (236-685) was kindly provided by C. Romanin (University of Linz, Austria) and S. Muallem (236-685; K680Q mutation; UT Southwestern, Dallas, TX) and HA-CT-STIM1 (237-685) by M. Cahalan (UC Irvine, CA). Orai1-ΔN, Orai1-ΔC and Orai1-ΔN73 were kindly provided by T. Xu (Chinese Academy of Sciences, Beijing, China). STIM1 or Orai1 fragments were amplified by PCR using the primer sets shown below. The PCR products were cloned into the pCR8 TOPO-adapted cloning vector (Invitrogen). The expression constructs were generated by transferring the pCR8 PCR products into destination plasmids using Gateway technology (Invitrogen). Sequences of all constructs were verified.

For STIM1 cyto 234-685 (CT-STIM1)
Forward AACCGTTACTCCAAGGAGCAC
Reverse GGAATTCCTACTTCTTAAGAGGCTTCTTAAAG

For STIM1 234-491
Forward AACCGTTACTCCAAGGAGCAC
Reverse TCACTGCATGGACAAGGGAGACAC

For STIM1 234-469
Forward AACCGTTACTCCAAGGAGCAC
Reverse TCAAGCAGGGTTGGGGCGTGTACTGCC

For STIM1 234-410
Forward AACCGTTACTCCAAGGAGCAC
Reverse GAATTCAATGATCTACATCATCCAGGGAAG

For STIM1 342-448 (CAD)
Forward GGATCCATGTATGCTCCAGAGGCCCTTC
Reverse GAATTCAGTGGATGCCAGGGTTGTTG

For STIM1 342-685
Forward GGATCCATGTATGCTCCAGAGGCCCTTC
Reverse GGAATTCCTACTTCTTAAGAGGCTTCTTAAAG

For STIM1 342-440
Forward GGATCCATGTATGCTCCAGAGGCCCTTC
Reverse TCACTGGAAGCCACAGAGGATCTCGAT

For STIM1 350-448
Forward GGATCCATGTGGCTGCAGCTGACACATGAG
Reverse GAATTCAGTGGATGCCAGGGTTGTTG

For STIM1 deltaCAD
Forward #1 CATGGTATGCTCCAGATATCCTTCAGAAGTGGCT
Reverse #1 AGCCACTTCTGAAGGATATCTGGAGCATACCATG

Forward #2 ATTGTCAACAACCCTGATATCCACTCACTGGTG
Reverse #2 CACCAGTGAGTGGATATCAGGGTTGTTGACAAT

For Orai1 1-91
Forward ATGCATCCGGAGCCCGCCCCGCCCCCG
Reverse TCACCGGCTGGAGGCTTTAAGCTT

For Orai1 1-70
Forward ATGCATCCGGAGCCCGCCCCGCCCCCG
Reverse TCAGGAGTGCTCGTTGAGGCTCAT

For Orai1 48-91
Forward GGATCCATGTCCGCCGTCACCTAC
Reverse TCACCGGCTGGAGGCTTTAAGCTT

For Orai1 48-70
Forward GGATCCATGTCCGCCGTCACCTAC

Reverse TCAGGAGTGCTCGTTGAGGCTCAT

For Orai1 68-91
Forward GGATCCATGGAGCACTCCATGCAGGCGCTG
Reverse TCACCGGCTGGAGGCTTTAAGCTT

For Orai1 142-177
Forward GGATCCACCTGCATCCTGCCCAACATCGAG
Reverse TCAGGCCCAGGCCAGCTCGATGTGGCG

For Orai1 255-301
Forward GGATCCGTCCACTTCTACCGCTCACTG
Reverse CTAGGCATAGTGGCTGCCGGGCGTCAG

For Orai1 E106A mutation,
Forward GTGGCAATGGTGGCGGTGCAGCTGGAC
Reverse GTCCAGCTGCACCGCCACCATTGCCAC

N-terminally myc-tagged WT Orai1 in the Gateway entry vector pENTR11 (a gift from S. Feske, Harvard Medical School, Boston, MA) was inserted into the custom-designed Gateway destination vector pDEST-pGWI by recombination reaction using enzyme mix (Gateway LR Clonase; Invitrogen, Carlsbad, CA) to generate pEX-pGWI-myc-Orai1.

After PCR amplification, CAD was cloned into the pCR8/GW/TOPO vector (Invitrogen) to yield pCR8-CAD. CAD and other products cloned into this vector were sequenced by using GW1 primer. Gateway LR clonase reactions (Invitrogen, Carlsbad, California) were used to generate YFP-CAD and Flag-myc-CAD using the destination vectors pDS-YFP-X (a gift from T. Meyer, Stanford University) and pDEST-pGWI-Flag-Myc-x vector (custom-designed), respectively.

Orai1 containing an extracellular HA epitope was constructed by insertion of the sequence GSGSYPYDVPDYAGSGS between aa 207 and 208 (G-Q) in the second extracellular loop of Orai1 using an XbaI and XhoI site (Prakriya et al., 2006). This construct was used to generate Orai1-ΔN, Orai1-ΔC and Orai1-ΔN73 using PCR amplification and cloning into the pCR8/GW/TOPO vector (Invitrogen). Gateway LR clonase reactions were used to generate YFP-extHA-Orai1 constructs using the destination vector pDS-YFP-x. All constructs were confirmed by sequencing. The primers used are shown below:

For Orai1 ΔNT
Forward TCCAGCCGGACCTCGGCTCTG
Reverse CTAGGCATAGTGGCTGCCGGGCGTC

For Orai1 ΔN73
Forward GGATCCATGGCGCTGTCCTGGCGCAAG
Reverse CTAGGCATAGTGGCTGCCGGGCGTC

For Orai1 ΔCT (1-256)
Forward GTCTTCGCCGTCCACTAGTACCGCTCACTGGTT
Reverse AACCAGTGAGCGGTACTAGTGGACGGCGAAGAC

Split-Ubiquitin Yeast Two Hybrid Assay
To generate fusion proteins with the N-terminal half of ubiquitin (Nub), full-length or fragments of Orai1 were amplified by PCR and cloned into the pDL2-Nubx vector (Dualsystems Biotech). The Nub sequence in the pDL2-Nubx plasmid contains a point mutation (NubG) that abolishes the spontaneous association of Nub to the C-terminal half of ubiquitin (Cub). The CAD was subcloned into the pAMBV4 vector, which contains Cub fused to a chimeric transcription factor consisting of the DNA binding domain from LexA and the VP16 transactivation domain.

GST-CAD Construct
To generate GST fusion proteins, CAD was subcloned into pGEX 6p-1 (GE Healthcare) and the pGEX-CAD was transformed into *E.coli* BL21 pRIL (Stratagene). Transformants were grown in liquid cultures under ampicillin selection and isopropyl-1-thio-β-D-galactopyranoside (IPTG, 1 mM) was added at an optical density of 0.5 at 600 nm. 3 h after IPTG induction at 30°C, cells were collected by centrifugation and resuspended in PBS containing protease inhibitors. The cells were sonicated, centrifuged at 12,000 rpm for 10 min at 4 °C, and the supernatant was incubated with glutathione sepharose 4B beads for 2 h. The recombinant proteins were eluted from the beads by incubation with glutathione elution buffer and subsequently dialyzed with PBS. Protein concentrations were measured by the Bradford method (Bio-Rad).

Cloning, Expression and Purification of EE-Orai1-His_8 and His_6-CAD
Orai1 was PCR amplified from eGFP-myc-Orai1 (described above) using primers that introduced an N-terminal EE epitope tag (sequence: EEYMPME) and a C-terminal His_8 tag. The PCR product was cloned in the pVL1393 insect expression vector using BamHI and NotI restriction sites. This construct was used to produce recombinant baculovirus via recombination with the baculovirus genome (Sapphire Baculovirus; Orbigen, San Diego, CA) after transfection into Sf9 insect cells. Recombinant EE-Orai1-His_8 was expressed by incubating Hi5 cells (Invitrogen, Carlsbad, CA) cultured in Insect-Xpress media (Lonza, Walkersville, MD) with the amplified recombinant virus for 48 h at 28 °C. The cells were harvested and lysed in the presence of protease inhibitors using a dounce homogenizer. Membranes were pelletted along with other cellular debris by centrifugation at 40,000 x g for 1 h at 4 °C, and solubilized by resuspension in a buffer containing 1% DDM (n-dodecyl-β-d-maltoside; Anatrace, IL, USA) and gentle rotation for 1 h at 4 °C. The unsolubilized material was removed by centrifugation at 40,000 x g for 1 h at 4 °C.

PCR-amplified CAD with an N-terminal His_6 tag was inserted in pVL1393 vector using BamHI and NotI sites, and baculovirus was generated as described

above. Hi5 cells were coinfected with His_6-tagged CAD and EE-Orai1-His_8 baculoviruses and harvested after 48 h. The cells were pelletted and solubilized using 1% DDM. His_6-tagged CAD and EE-Orai1-His_8 were purified together using Ni-NTA affinity chromatography followed by anti-EE precipitation. CAD coeluted with Orai1 even after extensive washing with buffer containing 0.5 M NaCl. The complex was then passed over a Superose 6 column under the same buffer conditions described for Orai1 alone. All buffers used for CAD contained 2 mM β-mercaptoethanol (β-ME).

Multi-angle Light Scattering (MALS)

For MALS analysis, the proteins purified after the Ni-NTA affinity step were concentrated using a 30 kDa cutoff vivaspin membrane and loaded on a Superose 6 column. Excess CAD eluted as a separate homogenous peak after the Orai1-CAD complex elution. A DAWN EOS light scattering system (Wyatt Technology, Santa Barbara, CA) equipped with a K5 flow cell, a 30-mW linearly polarized GaAs 690-nm laser, a pump (Model PU-980, Jasco Corp., Tokyo, Japan), and an HPLC Shodex KW-803 size exclusion column was used for determining the molar mass of CAD. The protein sample in running buffer (20 mM Tris pH 8, 150 mM NaCl, 10% glycerol, 0.02% DDM, 2 mM β-ME) was filtered through a 0.1 μm filter. 150 μg CAD was loaded at a concentration of 1 mg/ml. Both the light scattering unit and the refractometer were calibrated according to the manufacturer's instructions. A dn/dc value of 0.185 ml/g was used. Light scattering data was used from 11 detectors ranging from 50° to 134° (detectors 6 through 16). The detector responses were normalized against monomeric bovine serum albumin.

Patch-clamp Experiments

Pipette-membrane seals were formed in 2 mM Ca^{2+} Ringer's solution. After break-in to the whole-cell configuration, voltage stimuli consisting of a 100-ms step to -100 mV followed by a 100-ms ramp from -100 to + 100 mV were delivered every 5 s from the holding potential of +30 mV. After the currents reached a steady level (~300 s for wild-type STIM1), the external solution was changed via a multibarrel local perfusion pipette to a high-Ca^{2+} Ringer's containing (in mM) 130 NaCl, 4.5 KCl, 20 $CaCl_2$, 1 $MgCl_2$, 10 D-glucose, and 5 HEPES (pH 7.4 with NaOH). All data were leak-corrected using the current elicited in 20 mM Ca^{2+} Ringer's + 10 μM $LaCl_3$ at the end of the each experiment. $LaCl_3$ and 2-APB were added directly to parent solutions on the day of the experiment from 10 mM and 100 mM stocks in H_2O and DMSO, respectively.

Measurement of Orai1 Cell Surface Expression

HEK 293 cells were cultured on 10 mm coverslips and transfected with the extracellular HA-tagged Orai1 constructs as indicated. 16 h after transfection, the cells were fixed with 4% paraformaldehyde, 8% sucrose in PBS for 10 min in the absence or presence of 0.25% Triton X-100. After 1hr blocking with 3% BSA/PBS, cells were stained with anti-HA antibody (rat, 3F10; 1:1000 dilution in 3% BSA/PBS) for 2 hr at 4 °C, washed 5 times and detected with a secondary

goat anti-rat-Alexa 594 (1:1000 dilution, Molecular Probes). The ratio of YFP to HA-Alexa 594 fluorescence was measured in the whole cell using widefield epifluorescence microscopy. The cells were analyzed blind.

FRAP Analysis

FRAP recovery curves were analyzed with ImageJ (W.S. Rasband, NIH, Bethesda, MD, http://rsb.info.nih.gov/ij/), following a published method (Ellenberg et al., 1997) in which an empirical formula approximating the one-dimensional solution of the diffusion equation is fitted to the time course of fluorescence recovery within the bleached ROI. An offset was introduced to account for incomplete bleaching. The resulting equation,

$$I(t) = I_b + (I_f - I_b)\left(1 - \sqrt{\frac{w^2}{w^2 + 4\pi D t}}\right),$$

where *I(t)* is the mean intensity within the bleached region at time *t*, I_b is the intensity immediately after bleaching, I_f is the intensity after full recovery, *w* is the width of the bleached region, and *D* is the effective diffusion coefficient, was fit to the FRAP recovery curves with Igor Pro 5.0 (Wavemetrics) to determine *D*. Mobility was determined as $(I_f\text{-}I_b)/(I_0\text{-}I_b)$, where I_f and I_b are defined as above, and I_0 is the initial intensity within the ROI after correction for the loss of whole-cell fluorescence by the bleaching pulse (~10%).

Quantitation of STIM1 and Orai1 Recruitment into Puncta

Colocalization of eGFP-Orai1 and mCh-STIM1 variants was analyzed from background-corrected confocal image pairs acquired before and after store depletion. Puncta have two defining characteristics: (1) because they are sites of accumulation, STIM1 and Orai1 fluorescence intensities in puncta are greater than the respective mean intensities measured across the entire cell, and (2) because STIM1 and Orai1 co-localize in puncta, their fluorescence covariance is high. For each STIM1/Orai1 image pair, we computed the covariance of each pixel as $(S_i - s)(O_i\text{-}o)$, where S_i and O_i are the STIM1 and Orai1 fluorescence of pixel i, and s and o are the mean STIM1 and Orai1 fluorescence of the entire cell. A threshold criterion for puncta was set using the pre-depletion image pair. The mean and s.d. of the covariance values were calculated from pixels for which both S_i>s and O_i>o, and a covariance threshold was set equal to the mean + 2 x s.d. of this pre-depletion condition. Binary masks were applied to the pre- and post-depletion image pairs to isolate pixels for which S_i>s and O_i>o and whose covariance exceeds the pre-depletion threshold. Examples of the method are illustrated in Supplemental Fig. 6. Integrated STIM1 or Orai1 puncta intensity was calculated from the masked images and expressed as a fraction of the total fluorescence intensity in the unmasked image. Image analysis was carried out with ImageJ and the MacBiophotonics Intensity Correlation Analysis plug-in (http://www.macbiophotonics.ca/imagej/colour_analysis.htm).

Supplemental References

Ellenberg, J., Siggia, E. D., Moreira, J. E., Smith, C. L., Presley, J. F., Worman, H. J., and Lippincott-Schwartz, J. (1997). Nuclear membrane dynamics and reassembly in living cells: targeting of an inner nuclear membrane protein in interphase and mitosis. J. Cell Biol. *138*, 1193-1206.

Luik, R. M., Wu, M. M., Buchanan, J., and Lewis, R. S. (2006). The elementary unit of store-operated Ca^{2+} entry: local activation of CRAC channels by STIM1 at ER-plasma membrane junctions. J. Cell Biol. *174*, 815-825.

Prakriya, M., Feske, S., Gwack, Y., Srikanth, S., Rao, A., and Hogan, P. G. (2006). Orai1 is an essential pore subunit of the CRAC channel. Nature *443*, 230-233.

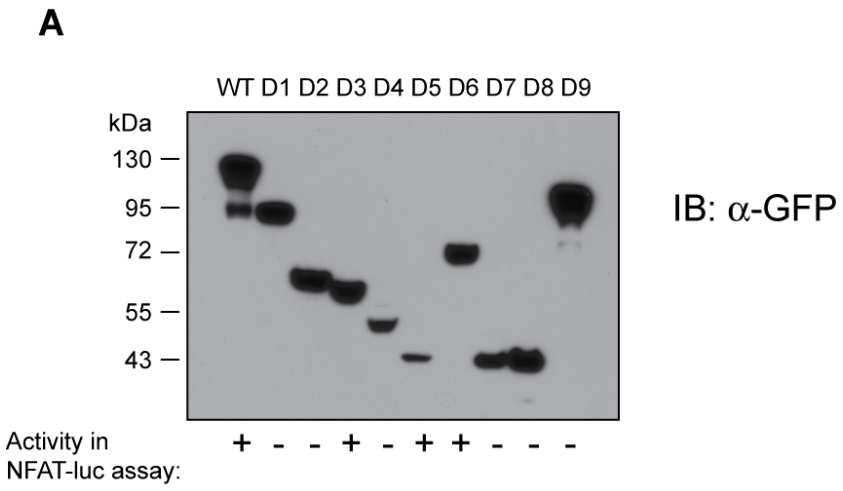

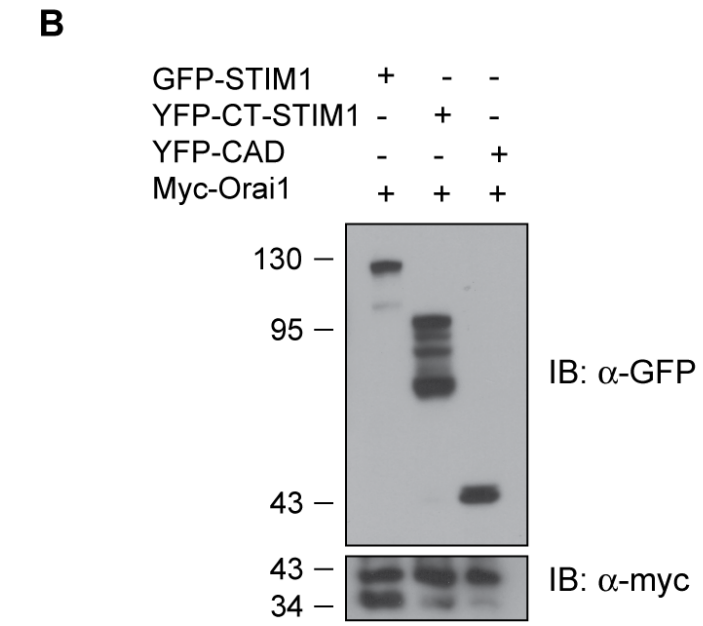

Figure S1. Expression of truncated STIM1 constructs. (A) HEK 293T cells were transfected with plasmids encoding YFP-tagged WT or truncated STIM1 constructs (D1-9 correspond to the diagrams shown in Fig. 2) and analyzed by Western blotting with anti-GFP antibodies. The ability of each STIM1 construct to activate an NFAT-luciferase reporter gene in the experiments of Fig. 2 is shown below the blot. Representative of 3 experiments. (B) Western blot of HEK 293 cells expressing myc-Orai1 together with GFP-tagged WT-STIM1, YFP-tagged CT-STIM1 or YFP-CAD. The upper panel shows expression of STIM1 proteins while the lower panel shows the expression of the Orai1 proteins (representative of 3 experiments).

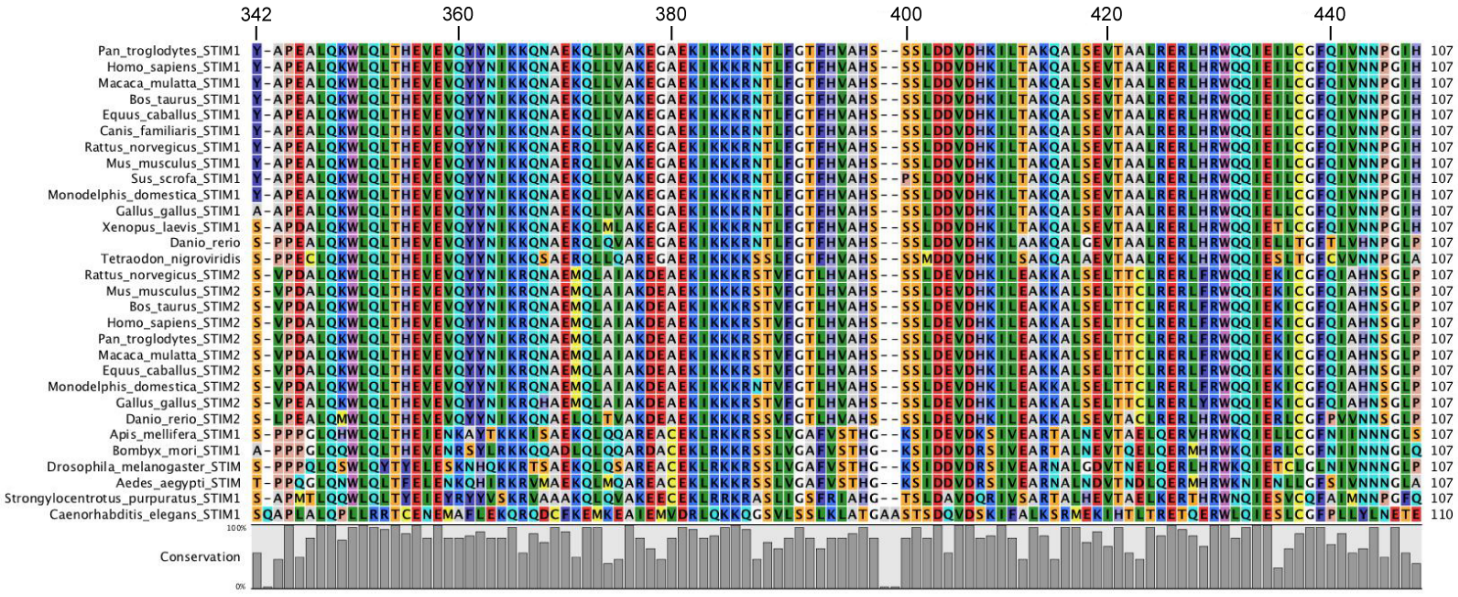

Figure S2. Sequence alignment of the CRAC activation domain (CAD) of STIM homologs. STIM1 and STIM2 sequences from vertebrate and invertebrate species were aligned with CLC Sequence Viewer v5.0 using default settings for gap penalties. The degree of conservation for each position is shown in the bar graph at bottom. Colors are standard Rasmol colors. Two gaps have been introduced to accommodate the *C. elegans* sequence. Accession numbers: *Pan troglodytes* STIM1 (XP_001160553.1), *Homo sapiens* STIM1 (NP_003147.2), *Macaca mulatta* STIM1 (XP_001112949.1), *Bos taurus* STIM1 (NP_001030486.1), *Equus caballus* STIM1 (XP_001499902.2), *Canis familiaris* STIM1 (XP_850663.1), *Rattus norvegicus* STIM1 (NP_001101966.2), *Mus musculus* STIM1 (NP_033313.2), *Sus scrofa* STIM1 (NP_001124446.1), *Monodelphis domestica* STIM1 (XP_001370519.1), *Gallus gallus* STIM1 (NP_001026009.1), *Xenopus laevis* STIM1 (NP_001090506.1), *Danio rerio* (NP_001038264.1), *Tetraodon nigroviridis* (CAF95381.1), *Rattus norvegicus* STIM2 (NP_001099220.1), *Mus musculus* STIM2 (CAN36430.1), *Bos taurus* STIM2 (XP_880249.3), *Homo sapiens* STIM2 (NP_065911.2), *Pan troglodytes* STIM2 (XP_001166811.1), *Macaca mulatta* STIM2 (XP_001084422.1), *Equus caballus* STIM2 (XP_001496930.2), *Monodelphis domestica* STIM2 (XP_001366125.1), *Gallus gallus* STIM2 (XP_420749.2), *Danio rerio* STIM2 (XP_692356.3), *Apis mellifera* STIM1 (XP_395207.3), *Bombyx mori* STIM1 (BAG68907.1), *Drosophila melanogaster* STIM (NP_523357.2), *Aedes aegypti* STIM (XP_001663818.1), *Strongylocentrotus purpuratus* STIM1 (XP_001186683.1), *Caenorhabditis elegans* STIM1 (Q9N379_CAEEL).

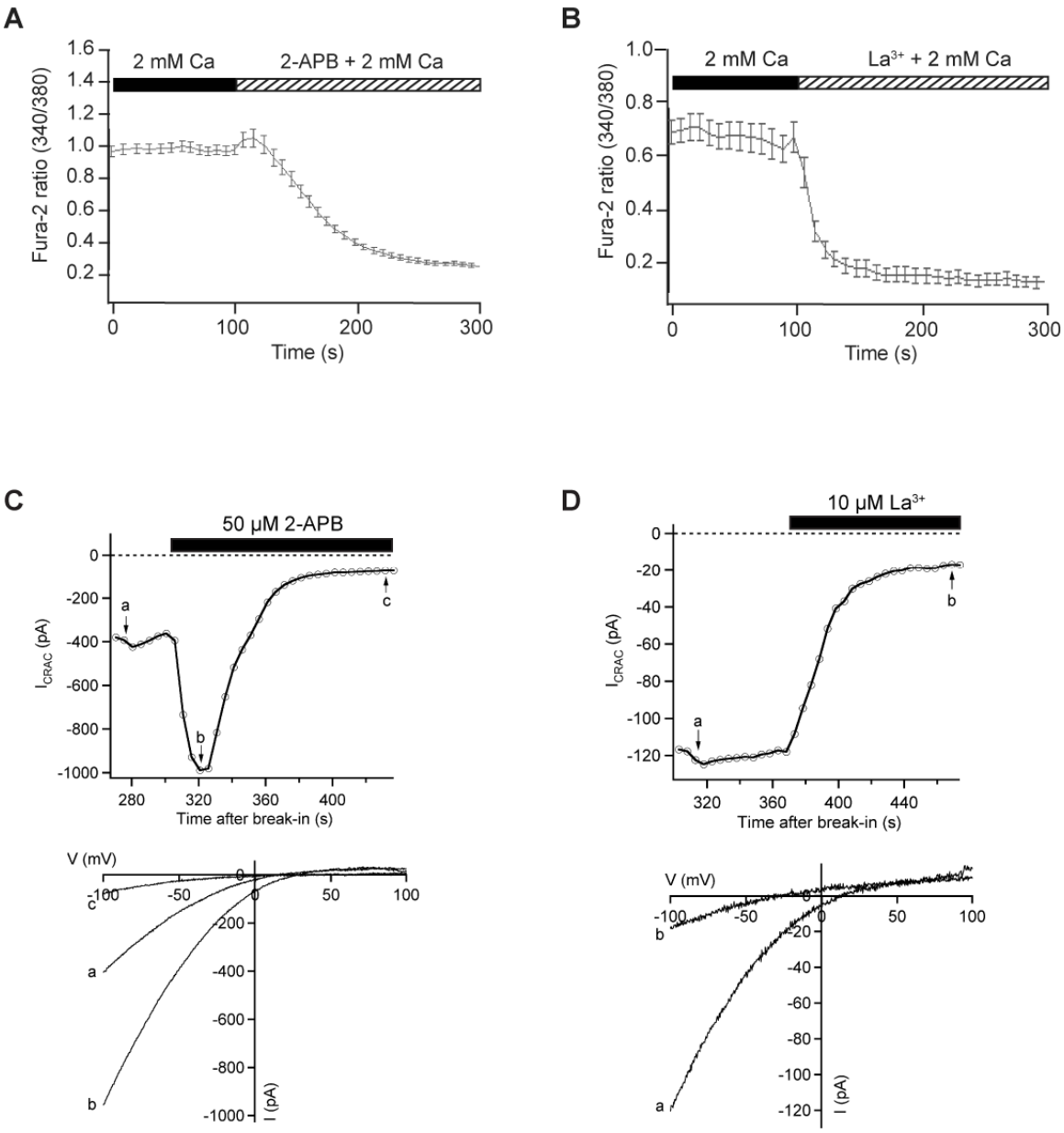

Figure S3. CAD-induced CRAC channel activity is Orai1-dependent and is sensitive to 2-APB and La^{3+}. Ca^{2+} imaging of HEK 293 cells expressing Orai1 and CAD shows a sustained elevation of $[Ca^{2+}]_i$ that is blocked by 100 μM 2-APB (A; n=19) or 10 μM La^{3+} (B; n=10). Data are shown as mean ± sem. (C) Effect of 2-APB on constitutive I_{CRAC} in a HEK 293 cell expressing YFP-CAD + myc-Orai1. 50 μM 2-APB was added in the constant presence of 20 mM Ca^{2+} to the bath as indicated. 2-APB causes an increase in CAD-dependent current followed by a slower inhibition, identical to the typical response of I_{CRAC} when activated through store depletion. Current ramps a-c below show the current-voltage relation before, immediately after, and >100 s after application of 2-APB. (D) Inhibition of CAD-supported current by 10 μM $LaCl_3$. This YFP-CAD + myc-Orai1 transfected cell in 20 mM $Ca^{2+}{}_o$ was perfused with 20 mM $Ca^{2+}{}_o$ + 10 μM

$LaCl_3$ at the time indicated by bar, leading to rapid inhibition of current. Traces are not corrected for leak current.

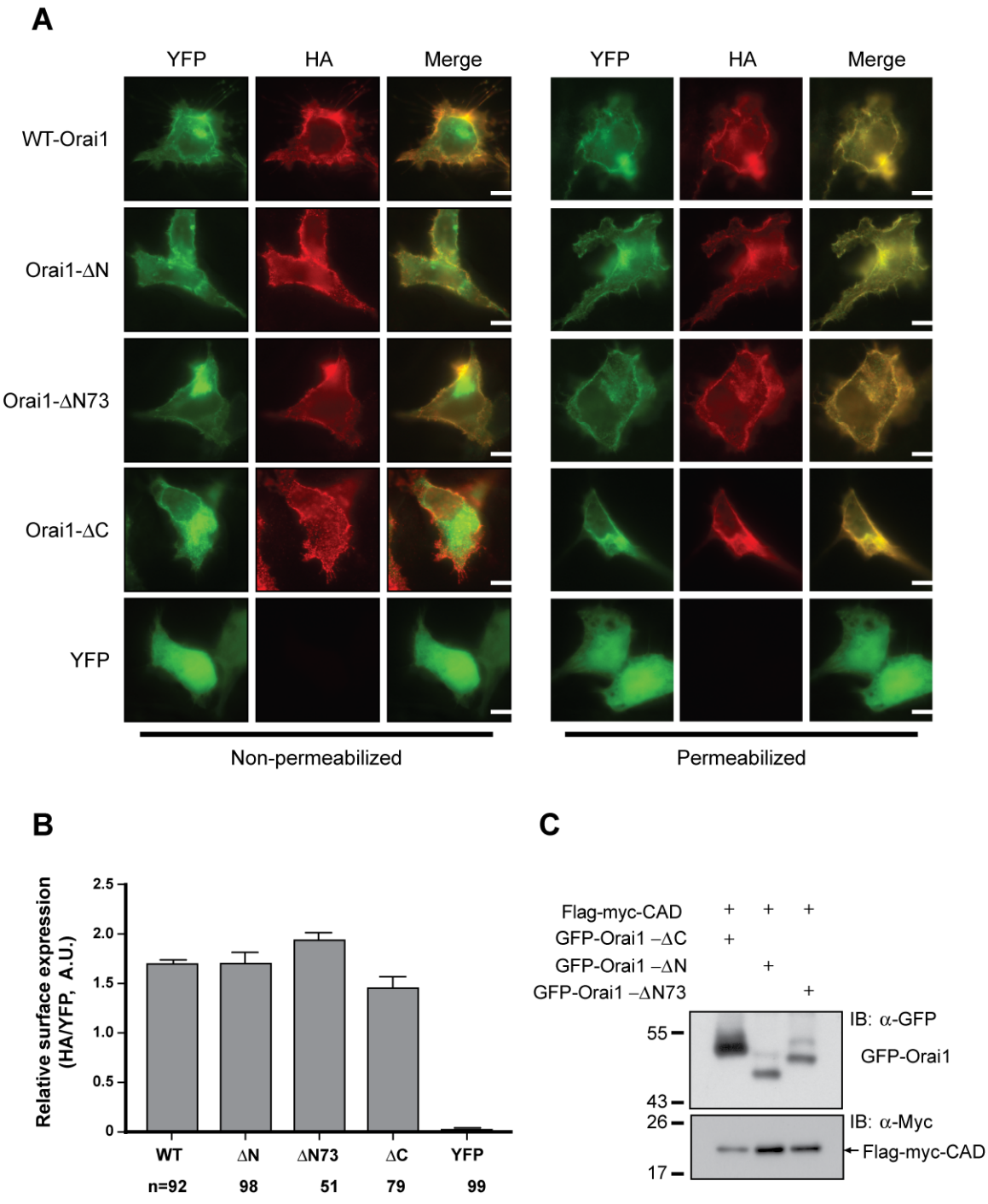

Figure S4. Cell surface trafficking and expression of Orai deletion constructs. (A) HEK 293 cells were transfected with either WT-Orai1 or the ΔN, ΔC or Δ73 Orai1 mutants containing an N-terminal YFP tag and an extracellular

HA tag. Fifteeen hours after transfection, the cells were fixed and stained with anti-HA antibodies prior to membrane permeabilization (left) or after permeabilization (right). In unpermeabilized cells, HA staining reflects cell surface Orai1 and YFP fluorescence reflects total expression of Orai1. (B) Quantification of cell surface Orai1 relative to the total expression of Orai1 in single cells (HA/YFP ratio) from the experiments shown in A. Data are shown as mean ± sem (number of cells indicated). (C) Western blot of HEK 293 cells transfected with Flag-myc-CAD and GFP-Orai-ΔC, GFP-Orai1-ΔN or GFP-Orai1-ΔN73 for 16 h. Anti-GFP antibodies show that GFP-Orai1-ΔC is expressed at slightly higher levels than ΔN or ΔN73 Orai1 (upper panel; n=3). Staining with anti-Myc antibodies (lower panel; n=3) shows that the CAD peptide is well expressed under all conditions. Small differences in the levels of CAD peptide in different conditions were not consistently observed (n=3).

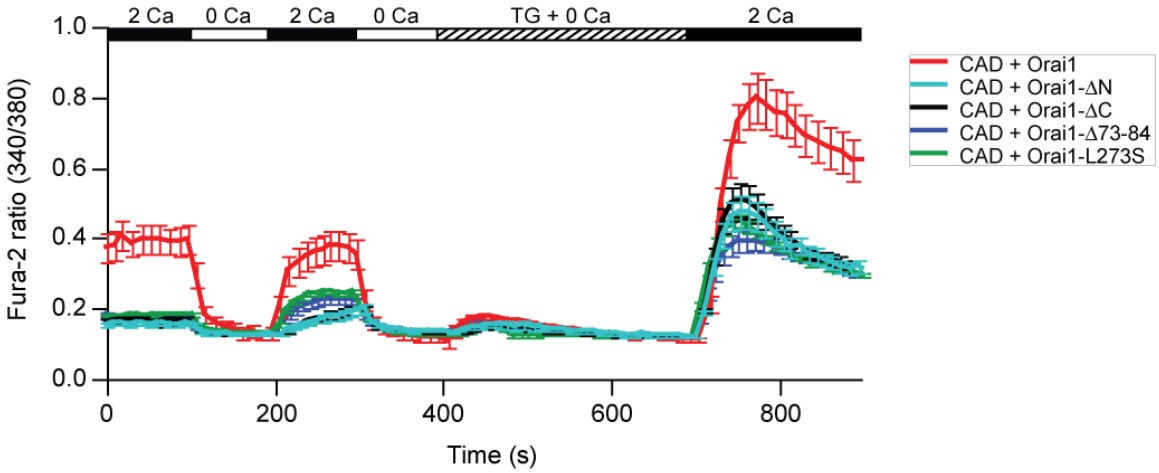

Figure S5. Deletion of aa 73-84 from Orai1 suppresses CAD-induced Ca^{2+} influx. Ca^{2+} imaging in HEK 293 cells expressing CAD and wild type Orai1 (n=9), Orai1-ΔN (n=15), Orai1-ΔC (n=22), Orai1-Δ73-84 (n=14; eliminates CAD binding to the N-terminus), or $Orai1_{L273S}$ (n=17; prevents CAD binding to the C-terminus). All of the mutations eliminate CAD binding sites and prevent activation of Orai1. All data presented as mean values ± sem.

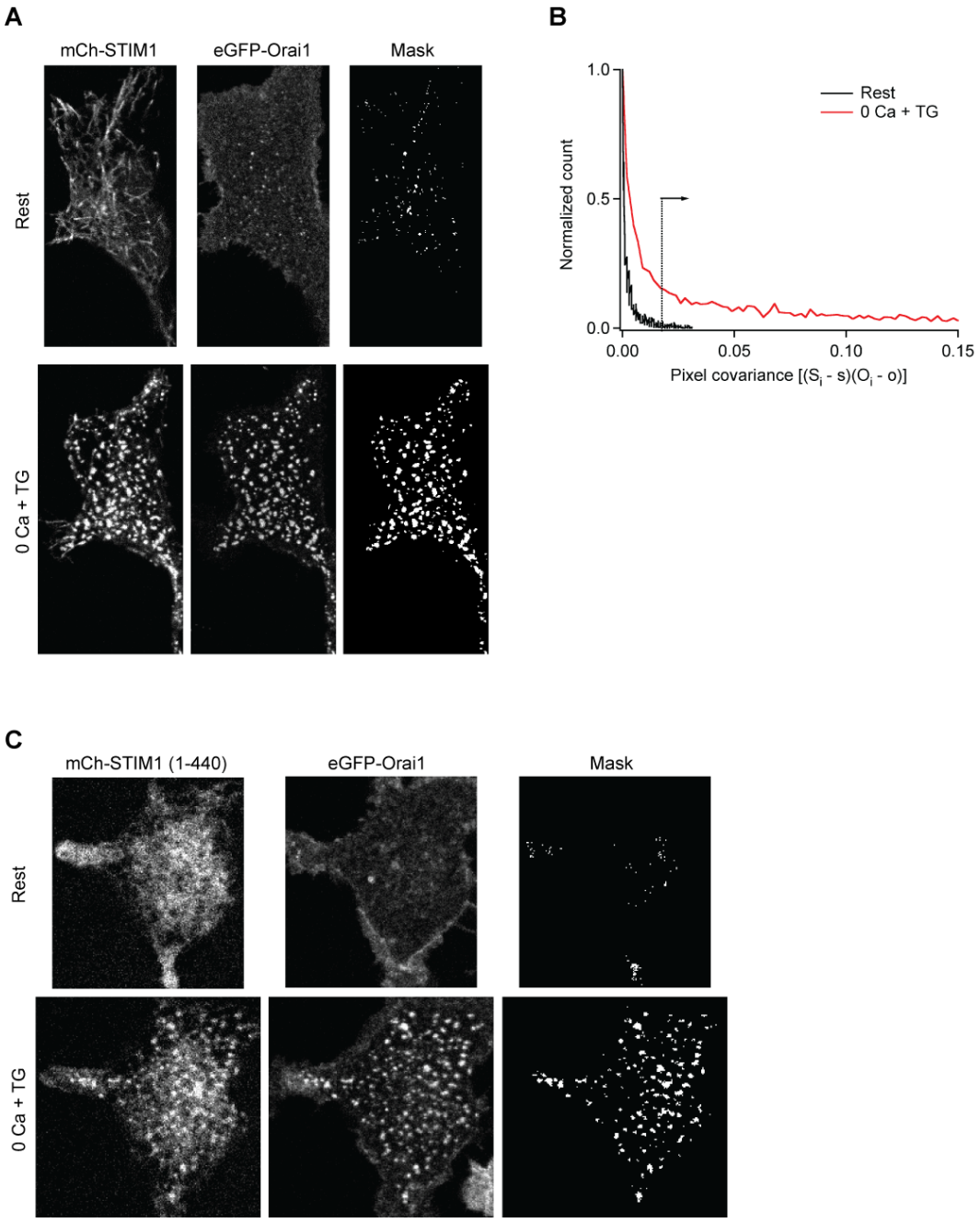

Figure S6. Covariance method for identifying puncta containing STIM1 and Orai1. (A) Confocal images of cells expressing mCh-STIM1 and eGFP-Orai1, before and after store depletion (from Fig. 1C). Pixels with covariance above threshold are used to generate binary masks which indicate the location of puncta where STIM1 and Orai1 colocalize. (B) Histograms of pixel covariance from the images in A before (Rest) and after (0 Ca + TG) store depletion. Each histogram is compiled from the covariance of pixels for which S_i>s and O_i>o, where S_i and O_i are the mCherry and eGFP fluorescence of pixel i, and s and o are the respective mean cell fluorescence values. The covariance threshold (dashed line) is set to two standard deviations above the mean covariance of the

resting cell. (C) Example of the covariance method applied to $STIM1_{1-440}$, in which a larger fraction of STIM1 remains in the bulk ER after store depletion. Puncta are identified accurately even against a higher background of diffuse ER fluorescence. Confocal images are from Fig. 7C.

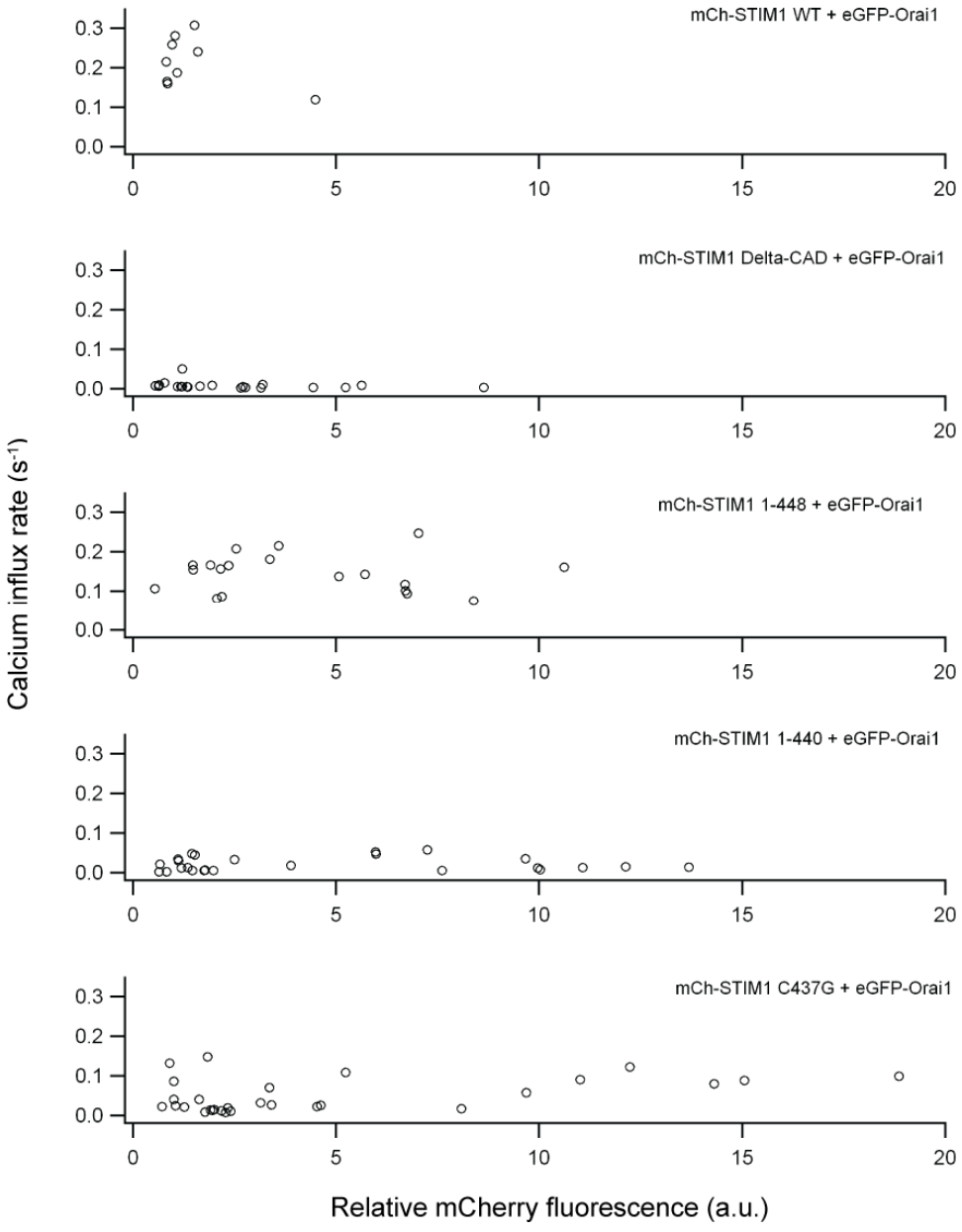

Figure S7. Relation of Ca^{2+} influx rates to the expression of STIM1 variants. For each cell whose Ca^{2+} response was measured in Fig. 7E, expression of the mCherry-labeled STIM1 construct was quantified by normalizing its fluorescence to that of a bath-applied standard rhodamine solution. This value is plotted for each cell against the Ca^{2+} influx rate expressed as dR/dt measured 10-20 s after

readdition of Ca^{2+} at 1100 s, where R is the fura-2 emission ratio with 350 and 380 nm excitation. Ca^{2+} influx is low or absent in STIM1-ΔCAD, $STIM1_{1-440}$, and STIM1 C437G despite expression levels similar to or greater than WT-STIM1. Relative GFP-Orai1 expression (mean ± sem) was also measured in cells coexpressing each STIM1 variant, from the single-cell GFP fluorescence normalized to the fluorescence of a standard fluorescein solution: 3.47 ± 0.34 (with STIM1, n=10), 2.41 ± 0.23 (with STIM1-ΔCAD, n=9), 3.87 ± 0.40 (with $STIM1_{1-448}$, n=12), 3.75 ± 0.44 (with $STIM1_{1-440}$, n=10), and 3.84 ± 0.26 (with STIM1 C437G, n=10). These data show that the lack of Ca^{2+} influx in cells transfected with STIM1-ΔCAD, $STIM1_{1-440}$, and STIM1 C437G are not due to abberrant expression of the STIM1 variant or Orai1.

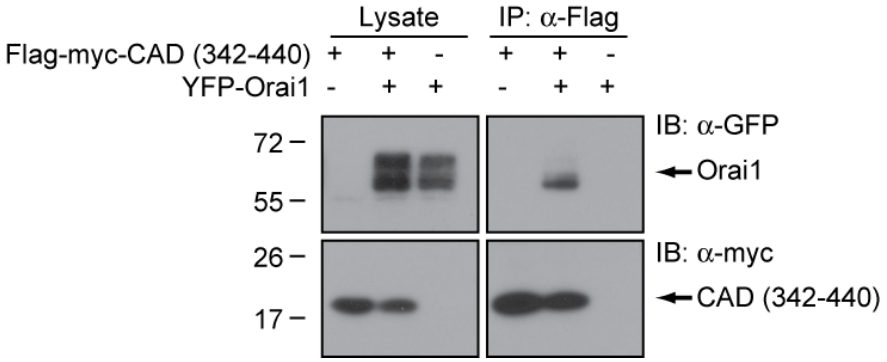

Figure S8. CAD (342-440) interacts with Orai1. YFP-Orai1 co-immunoprecipitates with Flag-myc-CAD (342-440) coexpressed in HEK 293 cells. Representative of 4 experiments.